

Identification of Extra-Framework Species on Fe/ZSM-5 and Cu/ZSM-5 Catalysts Typical Microporous Molecular Sieves with Zeolitic Structure

E.A. Urquieta-González, L. Martins, R.P.S. Peguin, M.S. Batista*

*Departamento de Engenharia Química, Universidade Federal de São Carlos,
Rodovia Washington Luís, Km 235, 13565-905 São Carlos – SP, Brazil*

Received: September 27, 2001; Revised: July 10, 2002

Cu and Fe species formed during the preparation of Cu/ and Fe/ZSM-5 catalysts by ion exchange were studied. XRD, SEM, H₂-TPR, DRS-UV-VIS, EPR, Mössbauer Spectroscopy (MÖSS) and chemical analysis (AAS) were used to sample characterization. Cu/ZSM-5 catalysts, irrespective of their Si/Al ratio and Cu content, showed a reduction peak at around 210 °C, which was attributed to the reduction of Cu⁺² to Cu⁺¹. The reduction peak of Cu⁺¹ to Cu⁰ shifted to higher temperatures with the increase of Si/Al ratio or with the diminution of Cu/Al ratio, evidencing that isolated Cu cations present a higher interaction with the zeolite structure. The MÖSS data showed the presence of Fe⁺³ species in charge-compensation sites and a higher content of hematite (Fe₂O₃) in the catalysts prepared in aqueous medium. The EPR analysis also evidenced the Cu⁺² and Fe⁺³ presence in Cu and Fe/ZSM-5 catalysts, respectively.

Keywords: *Cu/ZSM-5, Fe/ZSM-5, XRD, DRS-UV, H₂-TPR, EPR, Mössbauer Spectroscopy*

1. Introduction

In the last years metal/zeolites, crystalline aluminosilicates with properties and characteristics of microporous molecular sieves¹, have received more attention, as the possibility of their use as catalysts in environmental control processes and particularly in the nitrogen oxides (NO_x) reduction to N₂ in exhaust gases. For this process, the ZSM-5 zeolites, exchanged with metals, as Cu, Fe, Co, Ni, Mn, etc, have presented a higher catalytic activity than other zeolitic structures (FAU, MOR, BEA, etc)^{2,3,4}. Through the ion exchange property of zeolites⁵, it becomes possible to obtain catalysts having a metal of different type and content. After the ion exchange, the catalysts are submitted to a thermal treatment to allow the stabilization of the formed cationic metallic species, which will can present a different nature depending on the procedures utilized in their preparation⁶. The main interest in the studies of this kind of catalyst is the identification of the nature of the metallic species and the verification of their relation with its activity in the catalyst.

In the calcined metal exchanged zeolites, the active sites can be located principally in their internal channels and someone in the external surface of the zeolite crystallites. Therefore, the analysis and identification of these kind of

sites can result very complex, because, depending on the preparation methods utilized⁷, the metallic sites can be constituted by isolated cations and/or metallic species as (MeO-Me)⁺⁽²ⁿ⁻²⁾ oxocations or (MeO)⁺⁽ⁿ⁻²⁾ cations, with n being the metal valence. Crystalline or amorphous extra-framework metallic oxides deposited on the internal and on the external surface of the catalysts can also be present⁸. Then, the characterization techniques to be applied will must allow the identification of one particular physical or chemical property of those metallic species.

Hence, in the work reported here one or more techniques, as X-Ray Diffraction (XRD), Scanning Electron Microscopy (SEM), Electron Paramagnetic Resonance (EPR), Diffuse Reflectance Spectroscopy in the Visible Ultra Violet Spectrum (DRS-UV-VIS), Mössbauer Spectroscopy, Temperature Programmed Reduction with H₂ (H₂-TPR) and chemical analysis by Atomic Absorption Spectroscopy (AAS), were used to characterize ZSM-5 zeolites having cationic Cu or Fe species as charge-compensation cations of the zeolite structure.

2. Experimental

Catalysts Preparation

The Fe and Cu catalysts were prepared by sodium ex-

*e-mail: urquieta@power.ufscar.br

change in an aqueous medium from a Na/ZSM-5 zeolite having a Si/Al ratio of 11, 23 or 42. To obtain samples with different metal content, the time and the number of exchanges were varied. The Cu catalysts were obtained using a 0.015 mol/l solution of copper (II) acetate (Merck 99%) or using a 0.033 mol/l solution of FeCl₂ (Merck 99%) in the preparation of Fe/ZSM-5 catalysts. After ion the exchange, the samples were filtered, washed with deionized water and dried at 110 °C. Further, the samples were thermally treated at 520 °C (activation) under air flow during 1 h. The resulting Cu and Fe catalysts are showed in Tables 1 and 2, respectively.

To compare the methods of preparation, one sample of Fe/ZSM-5 catalyst (Table 2) was prepared by ion exchange in the solid state using an H/ZSM-5 zeolite as precursor, which had a Si/Al = 13. The H/ZSM-5 zeolite was mixed with FeCl₂ in an atomic ratio of Fe/Al = 0.37 and further activated for 6 h, being 2 h under N₂ flow and 4 h under air flow.

A reference sample, for to quantify the hydrogen consume during the H₂-TPR analysis, denoted as CuO/NaZ(11) (Table 1), was prepared mixing 2% w/w CuO with a Na/ZSM-5 zeolite (Si/Al = 11). It was further thermally treated during 1h at 520 °C under air flow.

The samples were denominated as Me(Y)Z(X), where Y (in %) represents the metal content (w/w) and X the Si/Al ratio of the zeolite, obtained from chemical analysis by atomic absorption spectroscopy (AAS). The sample

Fe/ZSM-5 prepared in the solid state was identified by the letter S: Fe(Y)Z(X)S.

Characterization

The structure and crystallinity of the ZSM-5, before and after the ionic exchange, were verified by XRD and the morphology of the Na/ZSM-5 was verified by SEM. H₂-TPR and DRS-UV-VIS were used to identify Cu species present in Cu/ZSM-5 samples. EPR analysis was used to identify the presence of Cu⁺² in Cu/ZSM-5 or Fe⁺³ ions in Fe/ZSM-5 catalysts. The presence of Fe⁺² or Fe⁺³ in Fe/ZSM-5 were verified using Mössbauer Spectroscopy.

The XRD patterns were obtained on a Siemens D500 Diffractometer using a monochromatic CuK α radiation. The XRD data were collected from 3 to 40°(2 θ) with a scanning rate of 2°(2 θ)/min. The SEM micro-analysis was performed on a Zeiss DSM 960 Scanning Electron Microscope operated at 30 kV. The H₂-TPR analysis were made on a Micromeritics Model 2705 equipment, having a thermal conductivity detector. It was used a H₂ flow of 30 ml/min (5% v/v in N₂), a dried sample of 150 mg and a speed heating of 10 °C/min. Before the analysis, the samples were thermally treated in air (30 ml/min) at 200 °C during 1h.

The DRS-UV-VIS spectra were obtained at room temperature on a UV-VIS Varian Cary 5G Spectrometer using a Teflon sample support, a quartz window and a politetrafluorethylene pattern as reference. Before the analysis, the samples were dried at 110 °C during 12 h. The obtained data were treated using the F(R) Schuster-Kubelka-Munk function⁹.

The EPR spectra were recorded in a Bruker ESP 300 E Spectrometer at -196 °C and the Mössbauer spectroscopy measurements were performed in the transmission geometry at room temperature and at -269 °C, using a 25 mCi ⁵⁷Co:Rh source moving in sinusoidal mode. The zero velocity was defined with respect to the centroid of the metallic iron spectrum, the source and the absorber being kept at the same temperature during the experiments.

3. Results and Discussion

Cu/ZSM-5 Catalysts

In Table 1 are showed the Cu content and the Cu/Al ratio in the samples. As can be seen, all the samples showed a smaller copper content than the possible maximum, which could be obtained when all the Na cations are exchanged (5.2 w/w% Cu for the Na/ZSM-5 with a Si/Al = 11). Supposing that all of the Cu atoms present in the samples are compensating the negative charge of the zeolite structure one can consider from the data given in Table 1, that the obtained samples present an exchange degree from 0 - 92%. However, it must be taken into account that the pH values

Table 1. Characteristics of the prepared Cu/ZSM-5 catalysts.

Sample	Exchange × Time (h)	Cu/Al	Cu (w/w%)
NaZ(11)	-	-	-
CuO(1.6)NaZ(11)	-	-	1.6
Cu(1.2)Z(11)	1/6	0.16	1.2
Cu(3.3)Z(11)	1/24	0.31	3.3
Cu(2.4)Z(11)	3/12	0.49	2.4
Cu(4.8)Z(11)	3/24	0.46	4.8
Cu(0.7)Z(23)	3/6	0.28	0.7
Cu(0.8)Z(42)	3/6	0.38	0.8
Cu(0.4)Z(42)	2/12	0.16	0.4

Table 2. Characteristics of the prepared Fe/ZSM-5 catalysts.

Sample	Exchange × Time (h)	Fe/Al	Fe (w/w%)
NaZ(11)	—	—	—
HZ(13)	3/8	—	—
Fe(1.1)Z(11)	2/6	0.15	1.1
Fe(6.7)Z(11)	3/24	0.90	6.7
Fe(2.9)Z(13)S	1/6	0.37	2.9

of the copper acetate solution before and after the ion exchange, were 5.5 and 5.3, respectively. This difference is attributed to the formation of $\text{Cu}(\text{OH})^+$ cations¹⁰ and/or precipitated $\text{Cu}(\text{OH})_2$, which will form CuO during the thermal treatment at high temperature. Therefore, without the determination of the nature of Cu species in the catalysts one cannot conclude that the Cu content showed in Table 1 represent all the Cu atoms in charge compensation sites. CuO presents diffraction hard peaks at $2\theta = 35.7^\circ$ and 38.5° , however, as can be observed in Fig. 1, the presence of this copper oxide in $\text{Cu}(3.3)\text{Z}(11)$ and $\text{Cu}(4.8)\text{Z}(11)$ samples was not detected by XRD. Moreover, the presence of CuO in the sample prepared with 2% of CuO , the $\text{CuO}/\text{NaZ}(11)$, is not clearly evidenced, as the peaks intensity is lower. Therefore, this result do not eliminate the possibility that non detectable crystallites or clusters of CuO with $d \leq 3$ nm were formed or their content in the samples is very low¹¹.

The SEM micrographs of the precursors, $\text{Na}/\text{ZSM-5}$,

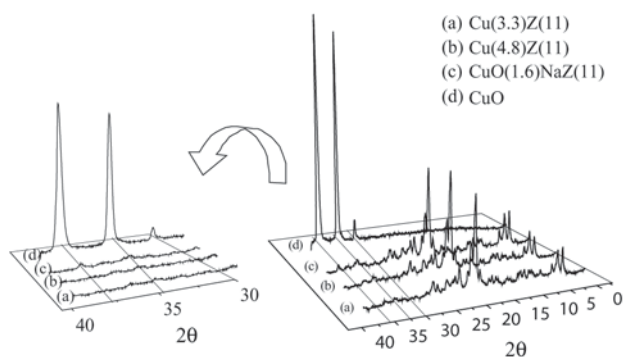


Figure 1. XRD patterns of $\text{Cu}(X)/\text{Z}(11)$ catalysts, $\text{CuO}/\text{Na}/\text{ZSM-5}$ and CuO .

are shown in Fig. 2. As can be seen, the zeolite having the lower Si/Al ratio is constituted by agglomerates of small crystallites, however, with the increase of this ratio, the crystals have the tendency to be isolated or geminates with a morphology of hexagonally prisms. As also observed by others authors^{12,13}, occurred an increase in the crystal size with the increase of the Si/Al ratio; this confirming the nucleation character of Al atoms in the synthesis medium.

Figure 3 shows the EPR spectra of two activated $\text{Cu}/\text{ZSM-5}$ samples having different Si/Al ratio. Since the Cu^{2+} ions in CuO or in $(\text{Cu-O-Cu})^{2+}$ species are silent for EPR^{14,15}, these spectra could only be assigned to isolated Cu^{2+} ions¹⁶. Both samples presented for the parallel component g_{\parallel} the value of 2.28 and averages A_{\parallel} values of 132 G for $\text{Cu}(0.8)\text{Z}(42)$ and 154 G for $\text{Cu}(1.2)\text{Z}(11)$. Modifications of the EPR parameters usually indicate changes in the Cu coordination, which can be a pyramidal or planar ligand field symmetry^{16,17}.

The H_2 -TPR profiles of $\text{Cu}/\text{ZSM-5}$ catalysts are presented in Fig. 4. The total hydrogen consumption showed a H_2/Cu molar ratio close to one. The samples, irrespective of their Si/Al ratio and Cu content, show a reduction peak at around 210°C , which can be associated to the reduction of isolated Cu^{2+} ions and the reduction of Cu^{2+} in oxocations, in both cases to Cu^{+1} . This low temperature peak can also contain the H_2 consumption corresponding to the reduction of Cu^{2+} in CuO to Cu^0 ^{11,18}. Already, the high temperature peaks ($> 350^\circ\text{C}$) correspond to the reduction of Cu^{+1} to Cu^0 . It is clearly seen from Fig. 4 that these peaks shifts to higher temperatures with the increase of Si/Al ratio of the zeolite, namely near to 580°C in $\text{Cu}(0.7)\text{Z}(23)$ and $\text{Cu}(0.8)\text{Z}(42)$. This is in accord with the redox properties of Cu cations, which are controlled by the local Si/Al ratio in the zeolite, then influencing their reducibility¹⁹. Therefore, the Cu cations in catalysts with higher Si/Al ratio, present a

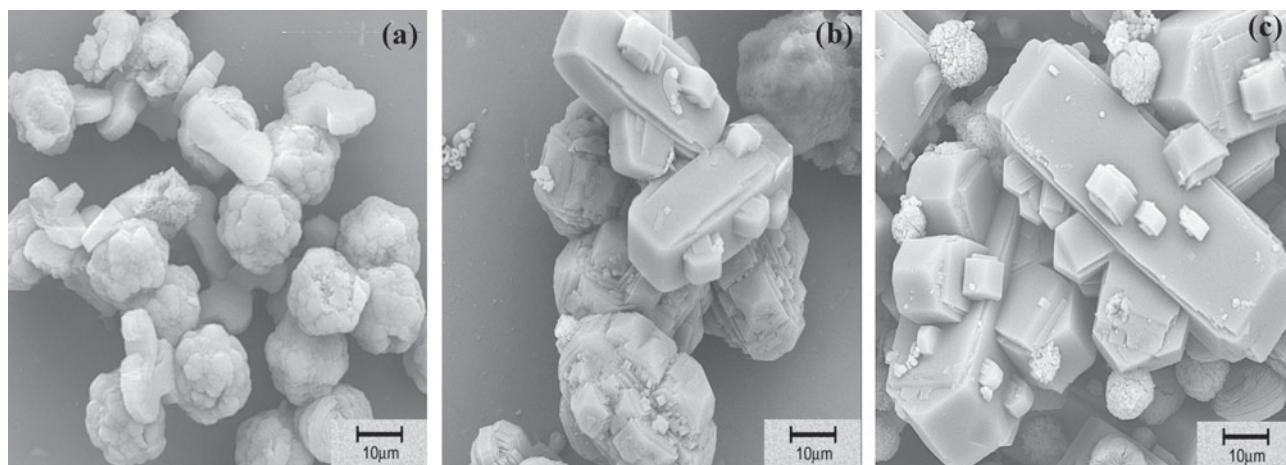


Figure 2. SEM micrographs of precursor $\text{Na}/\text{ZSM-5}$ having a Si/Al ratio equal to: (a) 11, (b) 23 and (c) 42.

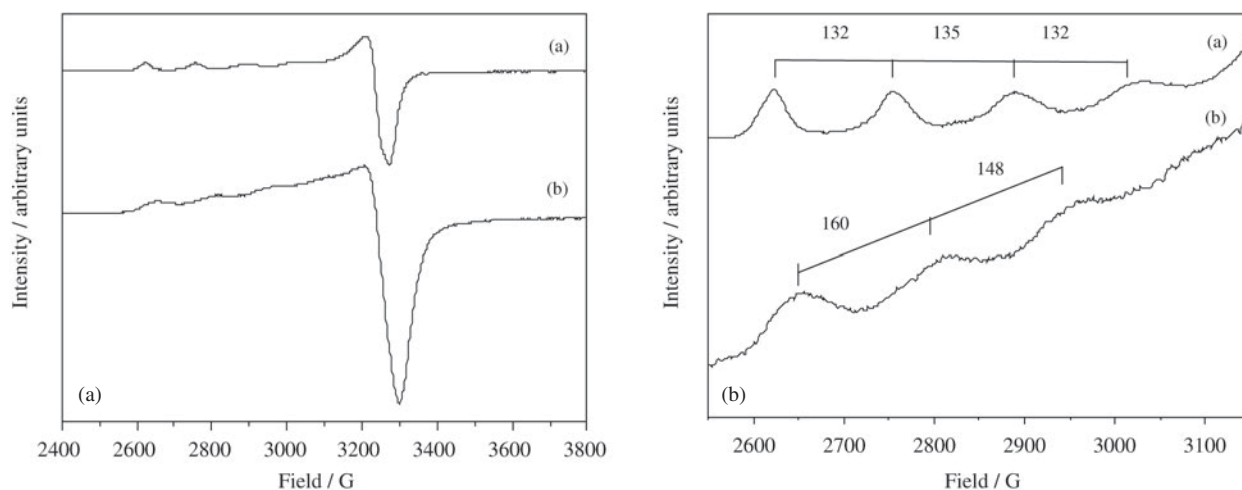


Figure 3. EPR spectra and copper hyperfine structure of: (a) Cu(0.8)Z(42) and (b) Cu(1.2)Z(11).

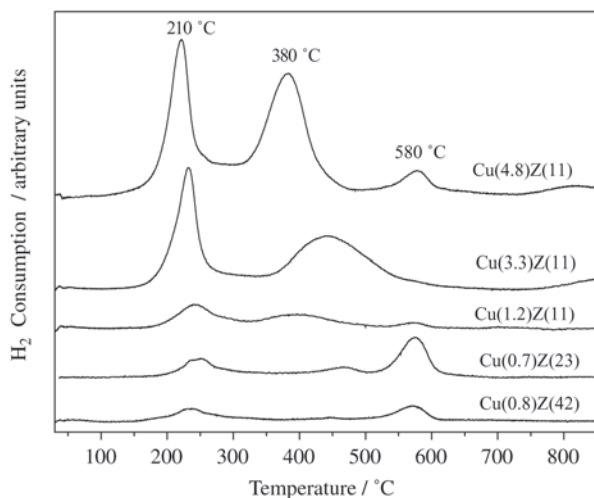


Figure 4. H₂-TPR profiles of Cu/ZSM-5 catalysts.

higher interaction with the zeolite structure and the capability to maintain at higher temperature the Cu cations in the +1 oxidation state.

In the DRS-UV-VIS spectra of some Cu/ZSM-5 catalysts (Fig. 5), it can be observed the presence of bands at 212, 256 and one broadest and low intense band in the range between 600 to 850 nm. As published by Itho *et al.*²⁰, the band at 212 nm, which is present in the spectrum of all samples, is correlated with the zeolite structure and therefore is not related with the Cu species present in the catalysts. The band at 256 nm has been attributed to Cu⁺² species interacting with the framework oxygen²¹ and those between 600 to 850 nm to Cu⁺² cations in hexagonal coordination²⁰⁻²¹.

Fe/ZSM-5 Catalysts

The Fe content and the Fe/Al ratio of the obtained Fe/ZSM-5 catalysts are shown in Table 2, which also shows the time and the number of applied ion exchange treatments. In the ion exchange in aqueous medium it was observed a decreases in the pH values, indicating a consumption of OH⁻ ions during the formation of iron species²².

The XRD patterns of all the iron-containing ZSM-5 showed the typical spectrum of MFI structure (Fig. 6). However, it was observed that the peak intensities decrease with the increase of Fe content. This decrease is attributed to the higher X-ray absorption coefficient of Fe compounds than Na compounds²³. No evidence of the presence of Fe₂O₃ (intense peak lines at $2\theta = 33.15^\circ$ and 35.65°) or any other phase beside ZSM-5 was found (Fig. 6).

The EPR spectrum of the Fe/ZSM-5 samples shows the presence of Fe⁺³, irrespective of the method used in the catalyst preparation. It is known that Fe²⁺ in aqueous solution is readily oxidized to Fe³⁺ by trace of O₂ unavoidably present. Therefore, even using a N₂ atmosphere during the ion exchange occurred the oxidation of Fe²⁺ to Fe³⁺, which at pH = 5.5 it can precipitate as α -FeOOH. In ion exchange in the solid-state, the oxidation of Fe²⁺ cations can occur during the physical mixing of reactants or during the thermal treatment. As above mentioned, the precipitation of α -FeOOH on the solid surface can generate solids with Fe/Al > 1/3, therefore, as occurred with the samples Fe(6.7)Z(11) and Fe(2.9)Z(13)S, the calculated exchange level resulted in a value higher than 100% (the close value for 100% Na⁺ exchange by Fe³⁺ cations is $(1/3)^2$). Such catalysts can hold outside of the zeolite framework one part of their Fe atoms in exchange sites and the rest as neutral species. During the activation, the precipitated α -FeOOH is

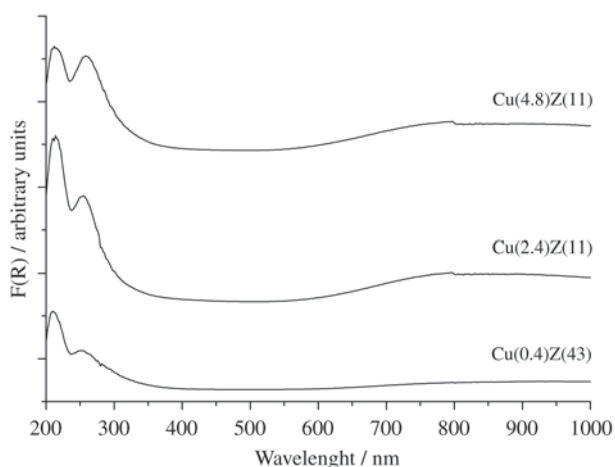


Figure 5. DRS-UV-VIS spectra of activated Cu/ZSM-5 catalysts.

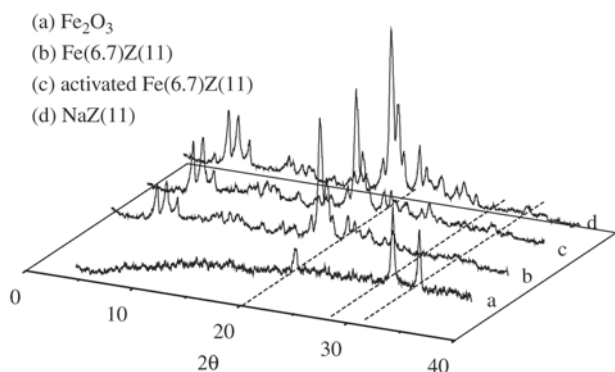


Figure 6. XRD patterns of: (a) hematite (Fe_2O_3); (b) and (c) Fe/ZSM-5 catalysts prepared in aqueous medium and (d) the precursor Na/ZSM-5.

dehydrated to form hematite. The Fe/ZSM-5 samples showed a g value of 4.29 for the activated Fe(1.1)Z(11) and a g value of 4.23 for the sample Fe(2.9)Z(13)S (Fig. 7). The difference in the lines of the spectra and therefore in g values is attributed to the different chemical environments of the Fe atoms. As described, in aqueous solution at a pH near 5.5, the Fe^{+3} form $[\text{HO}-\text{Fe}-\text{O}-\text{Fe}-\text{OH}]^{+2}$ species²⁴, which, similarly to the isolated Fe^{+3} cations, can also balance the negative charge of the zeolite. In the solid state method, the most probable charge-compensation species are FeCl_2^+ and FeO^+ cations²⁵.

In Table 3 are presented the data derived from Mössbauer spectra at -269°C shown in Fig. 8. Analysis of the samples at lower than room temperature was necessary, since at room temperature the magnetic hematite (present in the activated Fe(6.7)Z(11) and in the Fe(2.9)Z(13)S) and the magnetic

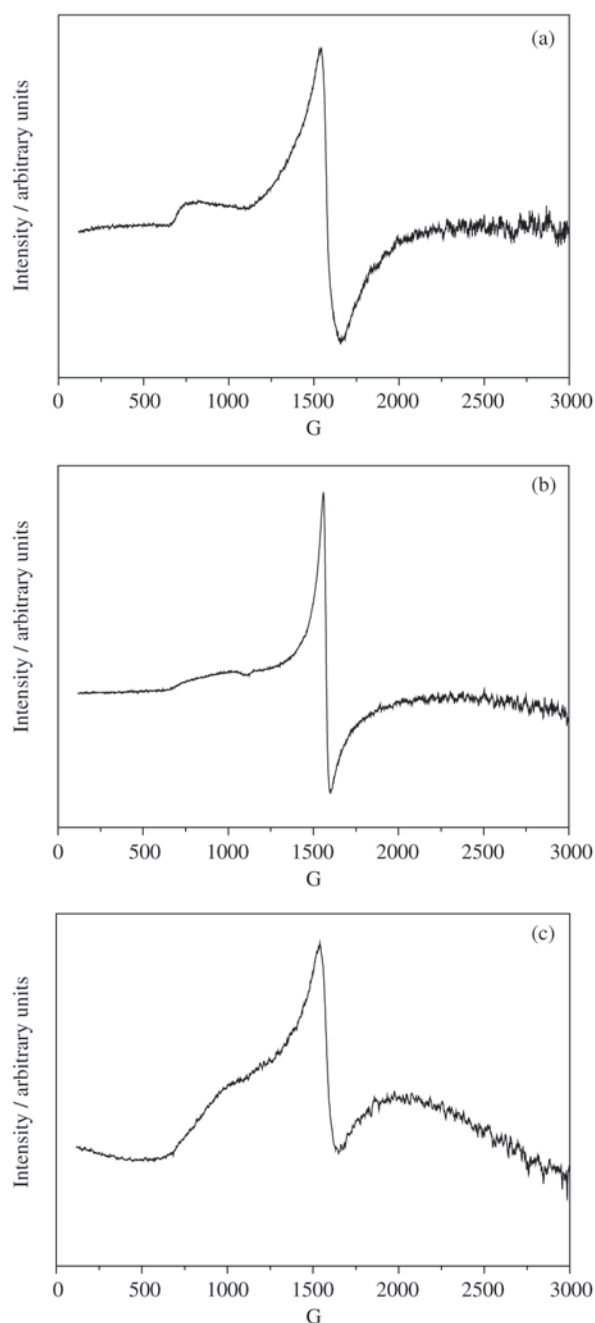


Figure 7. EPR spectra of (a) Fe(1.1)Z(11) after ionic exchange ($g = 4.28$); (b) Fe(1.1)Z(11) after activation at 520°C ($g = 4.29$) and (c) Fe(2.9)Z(13)S ($g = 4.23$).

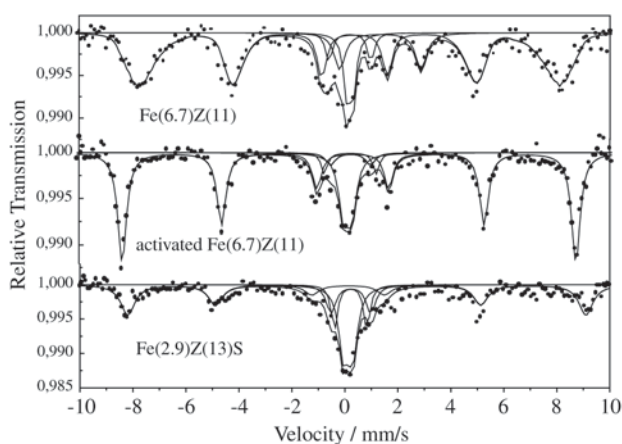
α -goethite (present in the non-activated Fe(6.7)Z(11)) exhibit only doublets, resulting at this temperature in a superposition with the paramagnetic doublets belonging to Fe species in charge-compensation sites^{26,27}.

It can be seen from the data in Table 3 that Fe^{+2} and Fe^{+3}

Table 3. Mössbauer spectroscopy data obtained from Fe/ZSM-5 zeolites at $-269\text{ }^{\circ}\text{C}$.

Sample	IS (mm/s)	QS (mm/s)	BHF (T)	AREA (%)	SITE
Fe(6.7)Z(11)	0.30	0.29	—	11	Fe ³⁺
	0.33	1.35	—	6	Fe ³⁺
	1.45	3.01	—	13	Fe ²⁺
	<0.37>	-0.25	<49.6>	70	GOETHITE
Activated Fe(6.7)Z(11)	0.25	0.30	—	6	Fe ³⁺
	0.34	1.20	—	19	Fe ³⁺
	0.35	-0.20	53	75	HEMATITE
Fe(2.9)Z(11)S	0.26	0.30	—	33	Fe ³⁺
	0.34	1.40	—	17	Fe ³⁺
	0.38	0.38	53.5	50	HEMATITE

IS: isomer shift related to α -Fe; QS: quadrupole splitting; BHF: magnetic field; relative AREA.

**Figure 8.** Mössbauer spectra of Fe/ZSM-5 catalysts obtained at $-269\text{ }^{\circ}\text{C}$.

ions coexist only in the as-prepared Fe(6.7)Z(11) catalyst. Fe²⁺ is transformed into Fe³⁺ during the thermal activation (see that Fe²⁺ is not present in the activated Fe(6.7)Z(11)). Therefore, the hyperfine parameters measured for the activated catalysts correspond only to species with Fe ions in the oxidation state +3, confirming the results obtained by EPR. The observed differences in the IS and in the QS values (Table 3) of cationic Fe³⁺ species can be attributed to different chemical environments. This is in agreement with the idea that outside of the zeolite framework coexist Fe³⁺ cationic species in charge-compensation sites and precipitated neutral iron compounds³, such as α -goethite before the thermal activation in as prepared Fe(6.7)Z(11) or as hematite in the latter catalyst after activation and in the catalyst prepared in the solid state.

In Table 3, the relative areas of the subspectra show that

70% of the Fe in the Fe(6.7)Z(11) sample is precipitated as α -FeOOH and 75% as Fe₂O₃ after thermal treatment. In contrast, the sample prepared in the solid state has only 50% of the Fe atoms as hematite and the remaining as Fe cationic species in exchangeable sites.

4. Conclusions

The Cu/ZSM-5 catalysts showed in the H₂-TPR analysis, a reduction peak at 210 °C, which was associated to the reduction of isolated Cu²⁺ ions and the reduction of Cu²⁺ in oxocations. The presence of Cu²⁺ was also detected by EPR and DRS-UV-VIS. The peaks corresponding to the reduction of Cu⁺¹ to Cu⁰ (> 350 °C), shifts to higher temperatures with the increase of the Si/Al ratio or with the decrease of the Cu/Al ratio. This fact was taken as an evidence of the presence of isolated Cu cations, which present a higher interaction with the zeolite structure and the capability to maintain at higher temperatures the Cu atoms in the oxidation state +1. This low temperature peak can also be associated to the reduction of Cu²⁺ to Cu⁰ in CuO, which was not detected by XRD.

The peaks in the XRD patterns of ZSM-5 structure, after the ion exchange of Na by Fe cations, were less intense than those of the precursor, the Na/ZSM-5; this providing evidence that Fe species were present in the catalysts. EPR analysis and Mössbauer spectroscopy indicated that all of Fe atoms present in the activated samples are in the oxidation state of +3, irrespective of the method used in the catalysts preparation. The Mössbauer data also showed that the catalysts prepared by both methods contain precipitated Fe species (such as α -FeOOH, after the ion exchange in aqueous medium, or as Fe₂O₃ in the thermally treated samples). However, the ion exchange performed in the solid state was the more promising, since the catalysts obtained by this method exhibited lower hematite concentration, thus hav-

ing a higher number of cationic Fe species in charge-compensation sites.

Acknowledgments

The authors gratefully acknowledge the Doctor's, Master's and Graduate's scholarships provided to Marcelo S. Batista by FAPESP (grant 98/02495-5), to Robson P. S. Peguin by CAPES and to Leandro Martins by FAPESP (grant 00/06176-3), respectively. The authors also gratefully acknowledge for the financial support for this study provided by CNPq (grant 461444/003) and to CBPF (Brazilian Center for Physical Research, Rio de Janeiro), LIEC (Electrochemical and Ceramics Inter-Disciplinary Laboratory, DQ/UFSCar) and IF (Physical Institute, USP, São Carlos) for the analysis and discussions of Mössbauer spectroscopy, DRS-UV-VIS and EPR, respectively.

References

1. Flanigen, E.M., *In: Introduction to Zeolite Science and Practice*, Stud. Surf. Sci. Catal., Elsevier, v. 58, p. 13-33, 1991
2. Li, Y.; Hall, W.K. *Journal of Catalysis*, v. 129, p. 202-215, 1991.
3. Yokomichi, Y.; Yamabe, T.; Kakumoto, T.; Okada, O.; Ishikawa, H.; Nakamura, Y.; Kimura, H.; Yasuuda, I. *Applied Catalysis B: Environmental*, v. 28, p. 1-12, 2000.
4. Iwamoto, M.; Hamada, H. *Catalysis Today*, v. 10, p. 57-71, 1991.
5. Townsend, R.P. *In: Introduction to Zeolite Science and Practice*, Stud. Surf. Sci. Catal., Elsevier, v. 58, p. 359-388, 1991
6. Satsuma, A.; Iwase, M.; Shichi, A.; Hattori, T.; Murakami, Y. *Progress in Zeolites and Microporous Materials*. Stud. Surf. Sci. Catal., Elsevier, v. 105, p. 1533-1540, 1997.
7. Wang, X.; Chen, H.; Sachtler, W.M.H. *Applied Catalysis B: Environmental*, v. 26, p. L227-L239, 2000.
8. Gervasini, A. *Applied Catalysis A: General*, v. 180, p. 71-82, 1999.
9. Perkampus, H.H. *UV-VIS Spectroscopy and Its Application*, SpringerVerlag, Berlin, Germany, p. 95-99, 1992.
10. Dossi, C.; Fusi, A.; Moretti, G.; Recchia, S.; Psaro, R. *Applied Catalysis A: General*, v. 188, p. 107-119, 1999.
11. Delahay, G.; Coq, B.; Broussous, L. *Applied Catalysis B: Environmental*, v. 12, p. 49-59, 1997.
12. Jahn, S.L.; *M. Sc. Dissertation*, Universidade Federal de São Carlos, 1987 (in portuguese).
13. Gaag, F.J.; Jansen, J.C.; Bekkum, H. *Applied Catalysis*, v. 17, p. 261-271, 1985.
14. Beutel, T.; Sárkány, J.; Lei, G.-D.; Yan, J.Y.; Sachtler, W.M.H. *Journal of Physical Chemistry*, v. 100, p. 845-851, 1996.
15. Yan, J.Y.; Lei, G.-D.; Sachtler, W.M.H.; Kung, H.H. *Journal of Catalysis*, v. 161, p. 43-54, 1996.
16. Soria, J.; Martínez-Arias, A.; Martínez-Chaparro, A.; Conesa, J.C.; Schay, Z. *Journal of Catalysis*, v. 190, 352-363, 2000.
17. Wichterlová, B.; Sobalik, Z.; Vondrová, A. *Catalysis Today*, v. 29, p. 149-153, 1996.
18. Sullivan, J.A.; Cunningham, J.; Morris, M.A.; Kencavey, K. *Applied Catalysis B: Environmental*, v. 7, p. 137-151, 1995.
19. Wichterlová, B.; Sobalik, Z.; Dedecek, J. *Catalysis Today*, v. 38, p. 199-203, 1997.
20. Itho, Y.; Nishiyama, S.; Tsuruya, S.; Masai, M. *Journal of Physical Chemistry*, v. 98, p. 960-967, 1994.
21. Feng, X.; Hall, W.K. *Journal of Catalysis*, v. 166, p. 368-376, 1997.
22. Moretti, G.; Dossi, C.; Fusi, A.; Recchia, S.; Psaro, R. *Applied Catalysis B: Environmental*, v. 20, p. 67-73, 1999.
23. Cullity, B.D., *Elements of X-Ray Diffraction*, 3th Ed., Addison-Wesley, USA, 1967.
24. Chen, H.Y.; Sachtler, W.M.H., *Catalysis Today*, v. 42, p. 73-83, 1998.
25. Karge, H.G.; Beyer, H.K. *In: Zeolites Chemistry and Catalysis*. Stud. Surf. Sci. Catal., Elsevier, v. 69, p. 43-64, 1991.
26. Abhaya, K.D.; Yaming, J.; Linda, M.; Thato, M.R.; Humphrey, D.T.; Neil, J.C. *In: Proceedings of the 12th International Congress on Catalysis*, Stud. Surf. Sci. Catal., Elsevier, v. 130, p. 1139-1144, 2000.
27. De Grave, E.; Vanderberghe, R.E. *Hyperfine Interactions*, v. 28, p. 643-646, 1986.